Unity Power Factor Control of Permanent Magnet Motor Drive System

M. F. Moussa* A. Helal Y. Gaber H. A. Youssef
(Arab Academy for science and technology) Alexandria University
*mona.moussa@yahoo.com

***Abstract*-The Permanent Magnet Synchronous motors (PMSMs) have gained an increasing interest recently. The wide variety of applications of PMSM drives makes it necessary to achieve fast and reliable drive control system design. Vector control of PMSM can achieve fast dynamic response with less complexity and parameter-independent controller, prevent demagnetization of the motor and allow maximum efficiency operation.**

In this paper, a novel Unity Power Factor (UPF) control drive for PMSMs is presented. The drive is performed with constraint on the (PF) such that its steady-state value is unity. This feature provides an extension of the constant torque region, resulting in higher output power of the PMSM drive, which is desirable in many applications requiring extended speed range at rated motor torque. However, this drive is not optimal in terms of efficiency which will be less than that obtained from conventional decoupled vector control drive for the same torque. Therefore, it is concluded that before reaching the rated speed, the conventional decoupled vector control is preferable, whereas, the UPF control is optimal to have a wider range of speed operation (above the base speed of the conventional vector control) and hence, extension of the constant torque region. Above this extended base speed, the PMSM drive can be operated in constant power mode using the conventional field-weakening technique having constant supply voltage and current. The drive system is built using MATLAB-SIMULINK software. The validity is evaluated in both steady-state condition and transient response using computer simulation.

***Keywords*-Unity power factor (UPF), permanent magnet synchronous motor (PMSM), vector control, oriented field control.**

I. INTRODUCTION

Recent developments in power semiconductor technology, digital electronics, magnetic materials and control theory have enabled modern AC motor drives to face challenging high efficiency and high performance requirements in industry. The permanent magnet synchronous motor PMSM is becoming popular in high performance applications compared to other types of AC motors due to its advantageous features including high torque to current ratio as well as high power to weight ratio, high efficiency, low noise and robustness [1]. Precise control of high performance (PMSM) over wide speed range is an engineering aspect. Motor's fast and accurate response and quick recovery of speed from any disturbances and insensitivity of parameter variations are some of the important characteristic of high performance drive system used in robotics, rolling mills, traction and spindle drive [2].

In this paper, a review of the conventional decoupled vector control drive system of PMSM is presented. In addition, a novel unity PF control system is described. The UPF control drive technique is explained and designed to achieve this constraint, by two methods: i) controlling the d-axis stator current i_d and ii) controlling the space angle of the command stator current i_s. Moreover, an improved steady-state analysis covering the power capability, voltage limit constraint, efficiency and power factor of the PMSM over wide speed range is also demonstrated. A comparison between the transient and steady state performances of the PMSM drive for both the unity power factor control and the conventional decoupled vector control techniques is investigated. The paper is organized as follows: section II presents the conventional decoupled control of PMSM. The novel control strategy achieving unity power factor is detailed in section III. Steady-state and transient performance analysis along with simulation results are demonstrated in sections IV and V respectively. Section VI presents conclusion of the paper.

The symbols used in this paper are as follows:

R_a	Stator resistance.
L_d, L_q	d-and q-axis inductances.
p	differential operator.
v_d, v_q	d-and q-axis components of stator voltages.
i_d, i_q	d-and q-axis components of stator currents.
ϕ_d, ϕ_q	d-and q-axis flux linkage.
T_e, T_L	Electromechanical and load torque.
β, J	Friction coefficient and moment of inertia.
ω	Electrical rotor angular speed.
ϕ_f	Constant flux linkage due to rotor permanent magnet.
P	Number of poles.
P_s,P_i,P_o	Stray losses, input power, and output power.
$\overrightarrow{\Phi_S}$,$\overrightarrow{e_S}$, $\overrightarrow{v_S}$	Space vector of stator phase flux linkage, e.m.f, and voltage.
$\overrightarrow{\Phi_L}$,$\overrightarrow{e_L}$, $\overrightarrow{v_L}$	Space vector of stator line-to-line stator flux linkage, e.m.f, and voltage.
$\overrightarrow{i_S}$	Space vector of line stator current.
i_a, i_b	Stator phase currents.
v_{ab}, v_{bc}	Stator line voltages.
$\overrightarrow{e_{LR}}$, $\overrightarrow{e_{LI}}$	Real and imaginary parts of line stator e.m.f.

$\overrightarrow{\phi_{LR}}, \overrightarrow{\phi_{LI}}$ Real and imaginary parts of line stator flux linkage.

$\theta_r, \theta_S, \theta_{\phi L}$ Rotor position, stator position, and space angle of the flux-linkage.

α_i, α_v Current and voltage angles.

ϕ, δ Power factor and load torque angles.

II. DECOUPLED CONTROL OF PMSM

The PMSM can be modeled where, the stator voltage equations in the rotor reference frame are expressed as follows [3]:

$$v_d = R_a\, i_d - \omega\, L_q i_q + L_d p i_d \quad (1)$$

$$v_q = R_a\, i_q + \omega\, L_d\, i_d + L_q p i_q + \omega \Phi_f \quad (2)$$

Also, the flux linkage equations can be written as:

$$\Phi_d = L_d\, i_d + \Phi_f \quad (3)$$

$$\Phi_q = L_q\, i_q \quad (4)$$

The electromechanical equation is given by:

$$T_e = \left(\frac{3}{2}\right)\left(\frac{P}{2}\right)\left[\Phi_f\, i_q + \left(L_d - L_q\right) i_q i_d\right] \quad (5)$$

The relationship between torque and speed is given by:

$$T_e - T_L = \left(\frac{2}{P}\right)\,(\beta\omega + Jp\omega) \quad (6)$$

Conventional control such as v/f control, may not meet high dynamic performance. However, decoupled vector control drive is used where the PMSM can achieve the dynamic performance capabilities of the separately exited DC machine, while retaining the general advantages of AC motors over DC motors. The basic principle of this control is based on field orientation. The stator current phasor in the d-q axis synchronously rotating frame has two components, namely the magnetizing current component and torque producing current component. The generated torque is the product of the two components. By keeping the magnetizing current component at constant value, the motor torque is linearly proportional to the torque producing component. In order to achieve maximum torque per ampere with linear characteristics, direct-axis current component i_d is forced to be zero resulting in the orientation of all the linkage flux in the d-axis [4]. Then, the reluctance torque is zero.

This control drive maintains maximum efficiency in a wide range of speeds and takes into consideration torque changes with transient response.

Substituting $i_d = 0$ (decoupled vector control condition) and $p = 0$ (operational term at steady-state), the general PMSM dynamic equations (1) to (5) tend to [3]:

$$v_d = -\omega\, L_q i_q \quad (7)$$

$$v_q = R_a\, i_q + \omega \Phi_f \quad (8)$$

$$\Phi_d = \Phi_f \quad (9)$$

$$\Phi_q = L_q\, i_q \quad (10)$$

And the electromechanical torque will be:

$$T_e = \frac{3}{2}\left(\frac{P}{2}\right)\Phi_f\, i_q \quad (11)$$

It should be noted that decoupling the d-q-axis components i_d and i_q, and enforcing i_d to be zero, minimum input power and hence, maximum efficiency operation can be achieved as follows:

The d-q stator voltages at steady-state are [4]:

$$v_d = R_a\, i_d - \omega\, L_q\, i_q \quad (12)$$

$$v_q = R_a\, i_q + \omega\, L_d\, i_d + \omega\, \Phi_f \quad (13)$$

The input power P_i is given by:

$$P_i = \frac{3}{2}\,(v_d\, i_d + v_q\, i_q) \quad (14)$$

The output power P_o is given by:

$$P_o = T_e\, \omega \left(\frac{2}{P}\right) - P_s \quad (15)$$

The efficiency $\eta = \frac{P_o}{P_i}$ (16)

To obtain maximum efficiency at the rated torque and speed (i.e. constant rated power), the input power is required to be minimum providing stray losses are almost constant. The suitable value of i_d which satisfies the condition of minimum input power P_i, and hence, maximum efficiency, can be obtained by differentiating P_i with respect to i_d and equating to zero, which yields:

$$i_d = \frac{\omega(L_q - L_d)\, i_q}{2R_a} \quad (17)$$

For cylindrical rotor which has identical rotor structure, substituting ($L_d = L_q$) into (17), to get:

$$i_d = 0 \quad (18)$$

This means that the maximum efficiency occurs when $i_d = 0$. In the same manner, the suitable value of i_d which satisfies the condition of maximum torque per ampere current ratio can be obtained by differentiating (11) with respect to i_d and equating to zero. Therefore, it was found that the maximum torque per current ratio occurs when $i_d = 0$.

Consequently, the decoupled vector control was found to be the optimal type of control in order to achieve maximum efficiency [5]-[9] and maximum torque per current ratio [10].

III. UNITY POWER FACTOR CONTROL

In some applications maximum realizable Power Factor (PF) is required during the operation of motor. A high performance unity power factor control (UPFC) for (PMSM) is proposed. Unity PF control is explained and the drive is designed to achieve this constraint, by two methods: i) controlling the d-axis stator current i_d and ii) controlling the space angle of the command stator current i_s.

UPFC strategy will allow wider range of constant torque region than decoupled vector control, by extending speed range above that of the conventional decoupled vector control, resulting in higher output power of the PMSM drive. That means UPFC permits a new speed range of operation, namely from the base speed of the normal decoupled vector control to the new extended base speed of the UPFC, which is desirable in many applications requiring extended speed range within constant torque region [11].

In a PMSM the direct control of rotor field is not possible. However, the field of direct-axis can be weakened by the demagnetizing effect of d-axis armature reaction current [7].

A. UPFC by controlling the d-axis stator current id

Unity power factor control implies that the VA rating of the inverter is fully utilized for real power input to the PMSM [11].

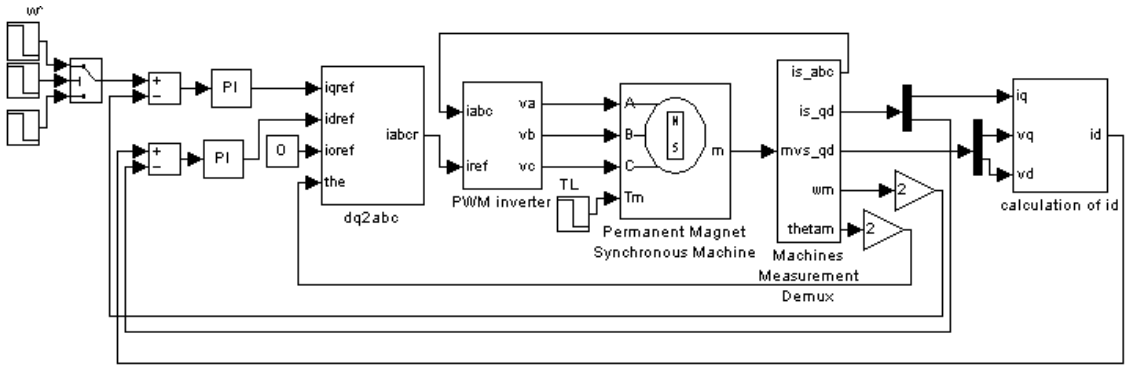

Fig. 1. UPFC scheme of the IPMSM drive by controlling the d-axis current.

This is enforced by controlling, i_d as a function of motor variables; so as to make the voltage and current in phase [6].

Since the armature current and voltage at steady-state are given by:

$$i_a = \sqrt{{i_d}^2 + {i_q}^2} \angle \tan^{-1} \frac{i_q}{i_d} \quad (19)$$

$$v_a = \sqrt{{v_d}^2 + {v_q}^2} \angle \tan^{-1} \frac{v_q}{v_d} \quad (20)$$

For unity power factor the phase angle of the current should equal the phase angle of the voltage, this implies that:

$$\frac{i_q}{i_d} = \frac{v_q}{v_d} \quad (21)$$

Therefore, $i_d = i_q \frac{v_d}{v_q}$ (22)

Equation (22) represents the necessary value of d-axis stator current which satisfies the condition of unity PF. Fig.1 shows the drive system of the UPFC for PMSM by controlling the d-axis stator current i_d.

The steady-state performance curves can be evaluated by applying the condition of UPFC of (22) into performance equations (12) and (13) such that they can be rearranged to get an expression of the q-and d-axis stator voltage at steady-state with unity power factor as follows:

$$v_q = \frac{\omega\Phi_f + 2i_qR_a \pm \sqrt{\left(\omega\Phi_f + 2i_qR_a\right)^2 - 4\left(\omega\Phi_f i_qR_a + \omega\Phi_f + \omega L_d L_q i_q^2 + i_q^2 R_a^2\right)}}{2} \quad (23)$$

$$v_d = \frac{\omega L_q i_q}{\left(\frac{i_q R_a}{v_q}\right) - 1} \quad (24)$$

The torque angle , can be calculated as:

$$\tan\delta = \frac{v_q}{v_d} \quad (25)$$

from which the torque angle is computed as:

$$\delta = \tan^{-1}\left(\frac{i_q R_a - v_q}{\omega i_q L_q}\right) \quad (26)$$

Note that the torque angle has to be less than 90º. Since, high torque angles will result in an increase of flux linkages contributing to saturation in the machine that is undesirable from losses point of view [11].

Having got v_q qnd v_d from (23) and (24), the value of i_d that satisfies unity power factor can be obtained from (22).

B. UPFC by controlling the phase angle of the stator current space vector

Another method of UPFC for PMSM can be applied where the phase angle of the command stator current is controlled such that the stator current space vector $\overrightarrow{\boldsymbol{\imath_S}}$ will be forced to have the same angle as the stator e.m.f space vector $\overrightarrow{\boldsymbol{e_S}}$. This will ensure that both voltage and current space vectors will coincide resulting in unity power factor. This can be explained as follows:

Since, $\overrightarrow{v_S} = \overrightarrow{e_S} + R_a\overrightarrow{\imath_S}$ (28)

Normally, it is practically easier to measure line voltage than phase voltage. Therefore, (28) is multiplied by $\sqrt{3}\, e^{j\frac{\pi}{6}}$, to get

$$\overrightarrow{e_L} = \overrightarrow{v_L} - \sqrt{3}\, R_a\overrightarrow{\imath_S}\left[\frac{\sqrt{3}}{2} + j\frac{1}{2}\right] \quad (29)$$

The line-line stator voltage vector $\overrightarrow{v_L}$ is given by [12]:

$$\overrightarrow{v_L} = v_{ab} + \frac{j}{\sqrt{3}}[v_{ab} + 2v_{bc}] \quad (30)$$

and the line current vector $\overrightarrow{\imath_S}$ is:

$$\overrightarrow{\imath_S} = i_a + \frac{j}{\sqrt{3}}[i_a + 2i_b] \quad (31)$$

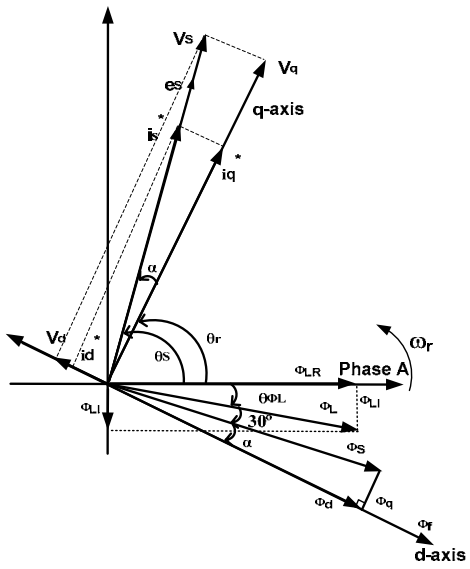

Fig. 2. Space vector diagram for UPFC of PMSM.

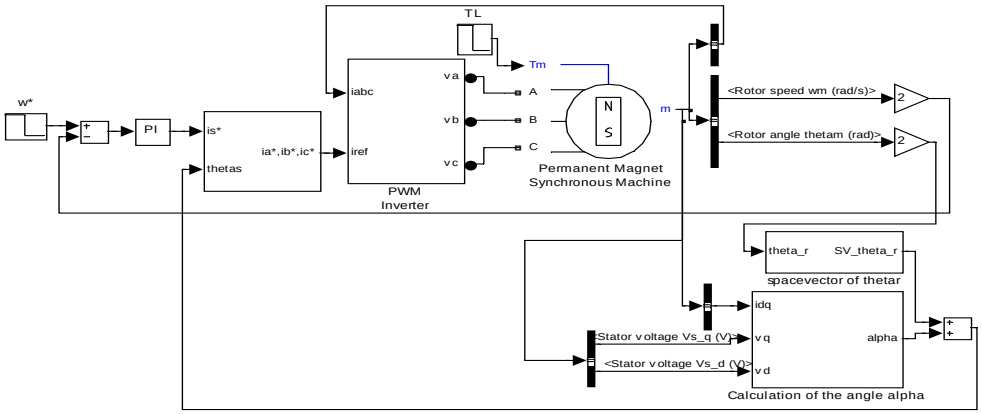

Fig. 3. UPFC scheme of the IPMSMS drive by controlling the angle of the stator current.

Substituting equation (30) and (31) into (29) yields

$$\overrightarrow{e_L} = e_{LR} + je_{LI} \quad (32)$$

where, $\overrightarrow{e_{LR}} = v_{ab} + R_a(i_b - i_a)$ (33)

$$\overrightarrow{e_{LI}} = \frac{1}{\sqrt{3}}[v_{ab} + 2v_{bc}] - \sqrt{3}R_a(i_a + i_b) \quad (34)$$

The line value of the flux linkage space vector $\overrightarrow{\phi_L}$ is related to the line e.m.f $\overrightarrow{e_L}$ by

$$\overrightarrow{\Phi_L} = \int \overrightarrow{e_L}\, dt = \Phi_{LR} + j\Phi_{LI} = \Phi_L \angle\theta_{\Phi L} \quad (35)$$

Since $\overrightarrow{e_S}$ leads $\overrightarrow{\Phi_S}$ by 90°, the stator current space vector $\overrightarrow{i_S}$ will be enforced to lead the stator phase flux linkage space vector $\overrightarrow{\Phi_S}$ by 90°, and since line value of flux linkage leads its phase value by 30°, the phase current space vector will lead line value of flux linkage by 60°.

The space angle of the flux-linkage is then given by:

$$\theta_{\Phi L} = \tan^{-1}\left(\frac{\Phi_{LI}}{\Phi_{LR}}\right) \quad (36)$$

$$\theta_S = \theta_{\Phi L} + 60^{\circ} \quad (37)$$

From the phasor diagram of Fig. 2, it is clear that the phase angle of the stator current $\overrightarrow{i_S}$ is leading the rotor angle (θr) by an angle α, which is the angle between the rotor frame (d-q frame) and the e.m.f frame, (β-γ frame). Thus,

$$\theta_S = \theta_r + \alpha \quad (38)$$

where, α is defined as the angle between the stator phase e.m.f $\overrightarrow{e_S}$ and the q-axis component of current i_q.

$$\alpha = tan^{-1}\left(\frac{\Phi_q}{\Phi_d}\right) \quad (39)$$

Consequently, by enforcing the phase angle θ_S of the stator current space vector $\overrightarrow{i_S}$ to be equal to the rotor angle θ_r plus the calculated angle α (between d-q frame & β-γ frame), a unity (PF) can be achieved over a wide range of speed and torque operation.

$$\overrightarrow{i_S} = i_S \angle\theta_S = i_S \angle\theta_r + \alpha \quad (40)$$

The drive system of the UPFC for PMSM by controlling the phase angle of the command stator current is shown in Fig. 3.

IV. STEADY-STAE ANALYSIS

The voltage supplied to the motor can be controlled by pulse width modulating the supply voltage up to a maximum value of modulation index corresponding to base value of motor speed.

A. For decoupled vector control

The base speed has been calculated by substituting (7) and (8) into (41).

Therefore, at base speed,

$$v_d^2(\omega_{base}) + v_q^2(\omega_{base}) = v_{a\_base}^2 \quad (41)$$

Where, $v_{a_base}$is the maximum voltage that can be obtained from the supply.

Substituting v_q and v_d from (7) and (8) into (41) and rearranging to get:

$$\omega_{base} = \frac{-b \pm \sqrt{b^2 - 4ac}}{2a} \quad (42)$$

$$a = \left(i_q L_q\right)^2 + \left(\phi_f\right)^2$$

$$b = 2 i_q \phi_f R_a \quad (43)$$

$$c = \left(R_a i_q\right)^2 - \left(v_{a\_base}\right)^2$$

After the base speed, the supply voltage and armature current equal to maximum permissible value v_{base} and i_{base} respectively.

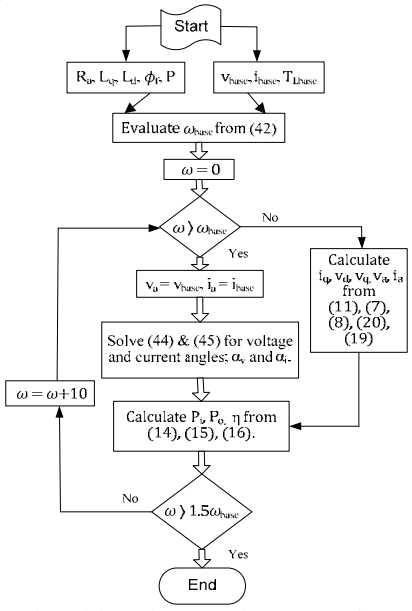

Fig. 4 Flow chart of the performance of vector control at steady-state.

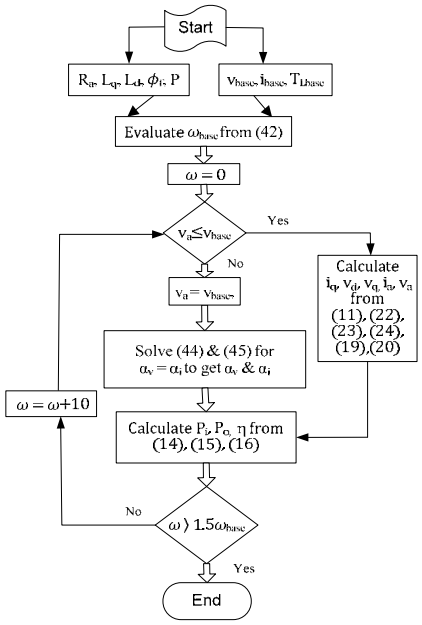

Fig. 5 Flow chart of the performance of UPFC at steady-state.

To get the d-q currents and voltages of the machine, when operating at field weakening above the base speed, (12) and (13) can be rewritten as:

$$v_a \cos\alpha_v = R_a\, i_a \cos\alpha_i - \omega\, L_q\, i_a \sin\alpha_i \quad (44)$$

$$v_a \sin\alpha_v = R_a\, i_a \sin\alpha_i + \omega\, L_d\, i_a \cos\alpha_i + \omega\, \Phi_f \quad (45)$$

For a certain speed, (44) and (45) can be solved for α_i and α_v.
Fig. 4 shows a flow chart to determine the performance of; the vector control at steady-state.

B. Steady-state at UPF

Similarly, for UPF control, the extended base speed can be also evaluated from (42), by substituting (23), (24), into (41).
Fig. 5 shows a flow chart to determine the performance of the machine for UPF control at steady-state.
The steady-state performance curves of the PMSM operation using the conventional vector control and the UPFC are shown in Fig. 6. The following observations are made:

- It is clear that the base speed in case of UPFC has increased by 25% above the base speed of the conventional vector control (from 680 rad/sec to 860 rad/sec). This means that the UPFC creates a new region which is considered as an extension of the constant torque region (see Fig. 6(b)). For UPFC, at 680 rad/sec (conventional rated speed), the phase voltage does not yet reach maximum supply voltage (155 volt), that means, it is still possible to inject more voltage to the motor before reaching its rated value resulting in higher output power of the PMSM. This feature is desirable in many applications requiring extended speed range within constant torque region [1]. However, this control strategy is not optional in terms of efficiency which will be reduced due to increased copper losses, hence the input power, to produce the same torque.
- It can be noted that, to obtain the same torque, more current is needed in case of the UPFC compared to the vector control, which can be considered as an advantage of the vector control, (see Fig. 6(a)).
- In the UPFC, after the extended speed, in order to make sure of getting unity power factor, higher current is needed. This is undesirable, since it may lead to overheating of the machine.
- It is clear that, in the vector control before the base speed (680 rad/sec), the d-axis component of current i_d will be zero, whereas, after the base speed, i_d will be negative. Consequently the field will be weakened in the d-axis since $\phi_d = \phi_f + i_d L_d$. This is what is known as field weakening [13], (see Fig. 6(c)).
- It can be concluded from the above steady state analysis that the machine can run in three modes of operations according to the speed such that; it is better to use the conventional decoupled vector control before reaching the base speed since it will give maximum efficiency (see Fig. 6(h)).

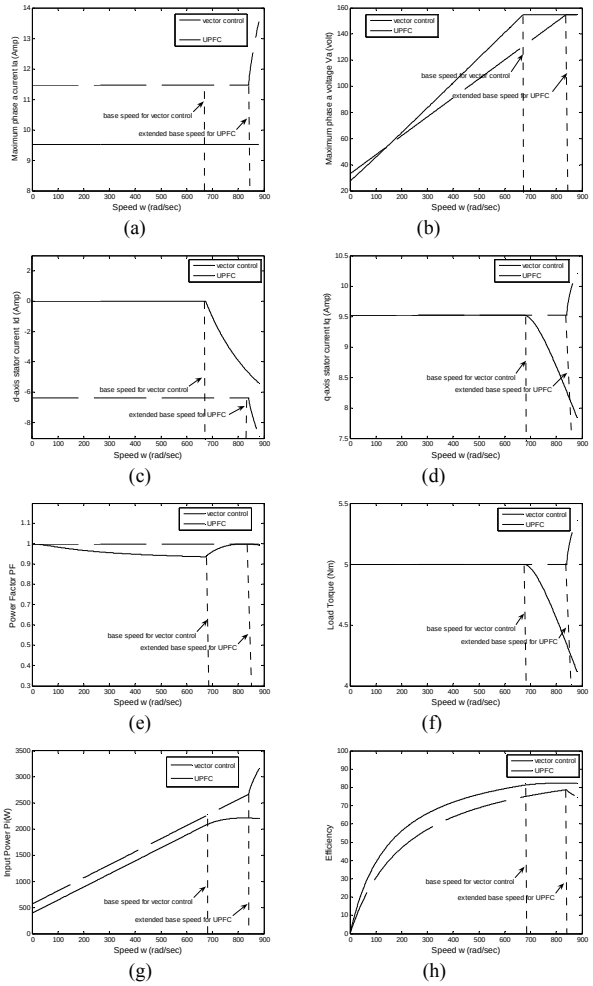

Fig. 6 Steady-state performances of both vector control & UPFC.

After this base speed, the UPFC is optimal in order to have a wide range of speed operation and hence, extensions of the constant torque region till the new base speed of the UPFC (see Fig. 6(f)). Above this extended base speed, the d-axis stator current i_d is increased (see Fig. 6(c)) with the increase of the speed in order to weaken the field and maintain almost constant power [8]. Consequently, the PMSM drive will operate in the constant power mode.

V. TRANSIENT RESPONSE

The transient performance of the drive system has been investigated using Matlab-Simulink. The simulated transient responses including the motor speed, d and q-axis command currents, phase-a-voltage, electromagnetic and load torque for step change of command speed at rated load for UPFC by controlling i_d with conventional vector control are shown in Fig. 7. The results have included both the constant torque and constant power regions. A step change of speed command from 500 (before base speed) to 700 rad/sec (after base speed) at time $t_1 = 0.2$ sec and then from 700 to 860 rad/sec (above base speed) at time $t_2 = 0.4$ sec is applied to both schemes; UPFC by controlling i_d and conventional vector control. For decoupled vector control, the time range before time (t_1) represents the constant torque region, while after time (t_1) is the constant power region. Whereas, for UPFC, the region from zero to time (t_2) is the constant torque region, where the phase voltage does not yet reach its rated value. After time (t_2) represents the field-weakening region.

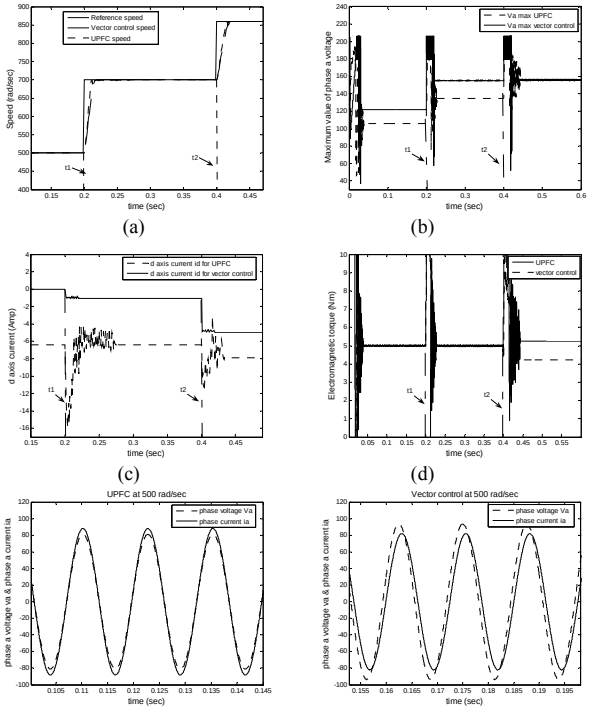

(a) (b) (c) (d) (e) (f)

Fig. 7 Simulated transient response for step change of speed at rated load using conventional vector control with UPFC by controlling i_d.

From Fig. 7, it can be noted that:

1- The electromagnetic torque T_e for the vector control is kept constant till time t_1 sec and then is reduced due to the increase of the speed in order to maintain constant power.

2- The region from time (t_1) to time (t_2) for conventional vector control is considered a field-weakening region during which, the power available is constant without exceeding the rated voltage of the machine. This means there will be progressively less torque available during this region [13]. Whereas, for UPFC, T_e remains constant in the region from 0 till time (t_2). And after time (t_2), the torque is decreased as shown in Fig. 7(e).

3- The reduction of the phase-voltage in case of UPFC means that there is more availability of voltage for wider range of speed operation before reaching the rated value as shown in Fig. 7(b).

4- In case of UPFC, the motor can develop more torque for the same stator current as compared with the vector control technique (see Fig. 7(d)). These features exhibit that for UPFC the motor can carry the higher load and still maintaining stability. It is also observed that for the same stator current the motor develops more torque at high speeds.

5- For vector control, in the constant torque region, i_q is almost constant, as it is proportional to the torque, but in constant power region, the torque producing component i_q decreases with the increase of speed in order to maintain the constant power while i_d becomes more negative to demagnetize the flux. Whereas, for UPFC, i_q is kept constant during the whole speed range of operation, and i_d is reduced negatively after time t_2 in the constant power region (see Fig. 7(c)).

The simulated transient responses including the motor speed with the electromagnetic and load torque for UPFC by controlling θ_S are shown in Fig. 8. A step change of speed command from 700 to 100 rad/sec at time $t_1 = 0.5$ sec and then a step change of load torque from 3 to 1 Nm at time $t_2 = 1$ sec is applied to the UPFC scheme demonstrated in Fig. 3.

It is evident from Fig. 7 and Fig. 8 that the motor can follow the command speed in both constant torque and power regions for both types of control schemes.

From Fig. 9, it can be noted that, the space vector of both the phase voltage and current coincide during the whole range of speed and torque operation.

In addition, Fig. 10 shows that the phase voltage is exactly in phase with the phase current.

Therefore, Fig. 9 and Fig. 10 demonstrate the unity PF operation over a wide range of speed and torque.

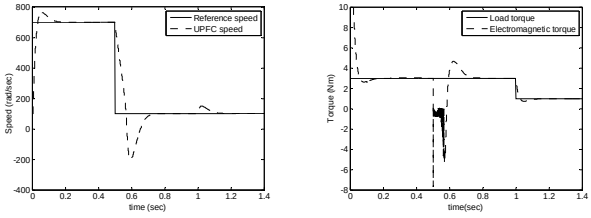

(a) (b)

Fig. 8 Simulated transient response for step change of speed at rated load using UPFC by controllingθ_S.

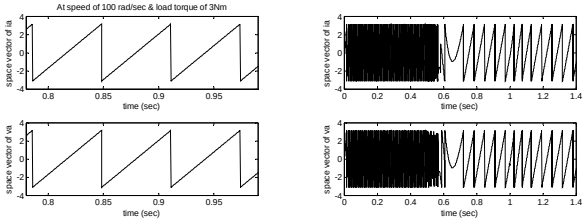

(a) (b)

Fig. 9 Space vector of phase voltage and current in case of UPFC by controlling θ_S: (a) At rated speed and torque, (b) At step change of speed and torque.

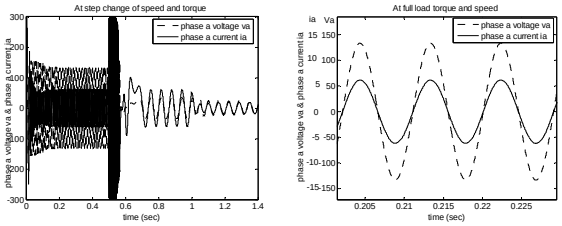

(a) (b)

Fig. 10 Maximum phase voltage and current in case of UPFC by controlling θ_S:(a) At step change of speed and torque, (b) At rated speed and torque.

VI. SYSTEM DESCRIPTION

TABLE I
3-ϕ SINUSOIDAL BACK-EMF PMSM
RATING AND PARAMETERS

R_a	2.875Ω
$L_d = L_q$	8.5mH
Φ_f	0.175 V/rad/s
n_{rating}	3000 r.p.m
T_{rating}	3 Nm
J	$0.8*10^{-3}$Kg-m^2
f	0.001Nm/rad/s
Power	1.1 kW
V_{rated}	220 V
frequency	50 Hz

VII. CONCLUSION

The performance of the PMS motor drive has been investigated for both vector control and unity power factor control techniques. The steady-state analysis of the drive has been presented. The analysis has included both the constant torque and constant power regions. It has been shown that both UPFC and vector control drives are stable for sudden change of command speed and load disturbances over a wide speed range. For the vector control drive, the maximum available speed is limited to a base value depends on the maximum supply voltage for constant torque operation. As for the UPFC, the base operating speed range for constant torque region has been extended significantly by about 25% over that of the conventional vector control, allowing the generation of a new region [from the base speed of the vector control to the extended base speed of the UPFC].

This region is considered as an extension of the constant torque region. That is why; this feature is desirable in many applications requiring extended speed range of operation. The reason of the creation of this extended region is that, the higher the power factor, the lower the voltage that can be obtained in order to keep the same current. This reduction of voltage in case of UPFC means that there is still more availability to increase the voltage for wider range of speed operation before reaching the rated value, while the phase current is kept constant. This means that, within this new constant torque region, the phase voltage does not yet reach its rated value. That is why; more voltage can be easily injected.

However, the analysis has indicated that this control strategy is not optimal in terms of efficiency which will be reduced by increased copper losses for the generation of same torque as compared to the conventional vector control that provides maximum efficiency. Moreover, the UPFC does not provide an important benefit from the power supply point of view as the voltage will decrease and not the current dislike in conventional power system. It was clear from the comparison between the steady-state performance of the conventional vector control and the UPFC that it is preferable to use the conventional vector control before reaching the base speed in order to obtain both; maximum efficiency and maximum torque per current ratio.

After this base speed, the UPFC is optimal in order to have a wide range of speed operation and hence, extensions of the constant torque region till the new base speed of the UPFC. Above this extended base speed, the PMSM drive can be operated in the constant power mode by increasing the d-axis stator current i_d according to the increase of the speed in order to weaken the field and maintain constant power. The performance of the complete drive system has been investigated using Matlab-Simulink, and the simulated results validate the improved analysis of the PMSM drive.

REFERENCES

[1] R. Krishman, "Selection criteria for servo motor drives", IEEE Trans. Ind. Appl., vol. IA-23, pp. 270-275, March/April 1987.

[2] T. S. Radwan, H. A. Rahman, A. M. Osheiba, and A. E. Lasine, "Performance of a hybrid current-controlled VSI-fed permanent magnet synchronous motor drives", in Pro-IEEE Pesc Conf. Rec, vol. 1, pp. 951-957, June 1996.

[3] B. K. Bose, power electronics and AC drives, Englewood cliffs, NJ: Prentice-Hall 1986.

[4] A. Nait Seghir, and M.S. Boucherit, "Adaptive Speed Control of Permanent Magnet Synchronous Motor", IEEE Trans. Ind. Electron., 2004.

[5] Christos Modemlis, Iordanis kioskeridis, and Nikos Margaris, "Optimal Efficiency Control Strategy for Interior-Permanent-Magnet-Synchronous Motor Drives", IEEE Trans. Energy Conv., vol. 19, no. 4, December 2004.

[6] Reza Fazai and Mahdi Jalili-Kharaajoo, "High Performance Speed Control of Interior-Permanent-Magnet-Synchronous Motors with Maximum Power Factor Operations", IEEE Trans. Ind. Appl., 2003.

[7] M. Nasir Uddin, Tawfik S. Ramadan, and M. Azizur Rahman, "Performance of Interior Permanent Magnet Motor Drive over wide speed range", IEEE Trans. Energy Conv., vol. 17, no. 1, March 2002.

[8] Jang-Mok Kim, Seung-Kisul, "Speed Control of Interior Permanent Magnet Synchronous Motor Drive for the Flux Weakening

Operation", IEEE Trans. Ind. Appl., vol. 33, no. 1, January/February 1997.
[9] Mahmoud I. Masoud, Jhon E. Fletcher, and Barry W. Williams, "Decoupled Control of Rotor Torque and Rotor Electric Power Delivered in a Salient-Pole, Synchronous Machine", IEEE Trans. Energy Conv., vol. 20, no. 1, March 2005.
[10] Christos Modemlis, and Nikos Margaris, "Loss Minimization in Vector Controlled Interior Permanent-Magnet Synchronous Motor Drives", IEEE Trans. Ind. Electron., vol. 49, no. 6, November/December 2002.
[11] P. Pillay and R. Krishnan, "Modeling Simulation and Analysis of Permanent-Magnet-Motor drives, Part. I: The Permanent-Magnet-Motor drive", IEEE Trans. Ind. Appl., vol. 25, no. 2, pp. 265-273, March/April 1989.
[12] Rusong Wu, and Gordon R. Slemon, "A Permanent Magnet Drive without a shaft encoder", IEEE Trans. Ind. Appl., vol. 27, no. 5, September/October 1991.
[13] Jang-Mok Kim, and Seung-Kisul, "Speed Control of Interior Permanent Magnet Synchronous Motor Drive for the flux weakening operation", IEEE Trans. Ind. Appl., vol. 33, no. 1, January/February 1997.